

Optical spectral weights and the ferromagnetic transition temperature of CMR manganites: relevance of double-exchange to real materials

A. Chattopadhyay¹, A. J. Millis² and S. Das Sarma¹

¹ *Department of Physics, University of Maryland
College Park, MD 20742*

² *Center for Materials Theory
Department of Physics and Astronomy, Rutgers University
Piscataway, NJ 08854*

(February 26, 2018)

We present a thorough and quantitative comparison of double-exchange models to experimental data on the colossal magnetoresistance manganese perovskites. Our results settle a controversy by showing that physics beyond double-exchange is important even in $\text{La}_{0.7}\text{Sr}_{0.3}\text{MnO}_3$, which has been regarded as a conventional double-exchange system. We show that the crucial quantity for comparisons of different calculations to each other and to data is the conduction band kinetic energy K , which is insensitive to the details of the band structure and can be experimentally determined from optical conductivity measurements. The seemingly complicated dependence of T_c on the Hund's coupling J and carrier concentration n is shown to reflect the variation of K with J , n and temperature. We present results for the optical conductivity which allow interpretation of experiments and show that a feature previously interpreted in terms of the Hund's coupling was misidentified. We also correct minor errors in the phase diagram presented in previous work.

I. INTRODUCTION

The colossal magnetoresistance (CMR) rare earth manganese perovskites first attracted attention in the 1950s because of the range of magnetic and structural transitions they display. Recent interest has been revived by the extremely large ("colossal") magnetoresistance displayed by some CMR materials, coupled with their rich phase diagram¹. Despite this long and intense study, much of the physics of CMR remains controversial, with basic issues still subject to debate. In this paper we address two such issues: the first is in what sense the standard 'double-exchange only' model (defined below) describes the physics in the regions of the phase diagram where the ground state is a ferromagnetic metal. The second is the interpretation of the optical conductivity spectrum, and in particular which portions of the observed spectrum pertain to the conduction band electrons responsible for the interesting physics of the CMR materials. In addition to its direct relevance to CMR, we believe our work is of broader significance for the theory of interacting electrons in solids, as a contribution to the fundamental issues of the quantitative comparison of many-body calculations to the properties of materials, and to the interpretation of the optical spectra of correlated electron materials.

It is generally agreed that a crucial aspect of CMR physics is 'double-exchange'²: the mobile carriers (which, for CMR materials, are $Mn e_g$ symmetry d -electrons) are strongly coupled ferromagnetically to localized core spins ($Mn t_{2g}$ symmetry electrons). This means that core spin alignment dictates carrier motion, which in general leads to ferromagnetism. What, if any, additional physics be-

yond double-exchange is important for the manganites is still debated¹. For example, some authors have argued that double-exchange only models correctly predict the magnetic transition temperatures of CMR materials^{3,4}, while others have argued that they do not^{5,6}. Published calculations of T_c ^{3,7} have not resolved the issue because the results depend on model parameters such as bandwidth, interaction strength and carrier density, often chosen arbitrarily or in a manner inconsistent with the physics of the manganites. We attempt to settle the question by establishing the full phase diagram and by presenting precise calculations of T_c within a specific model. Most importantly, by showing how the parameters on which the calculated T_c depends can be related to measured properties of real materials and to parameters used in other calculations.

Another important set of issues concerns the optical conductivity, which in the CMR materials has a strong dependence on chemical composition, frequency, temperature and magnetic field^{1,8-12}. It is widely believed that information extracted from these data will be helpful in elucidating the physics of CMR, but this goal has not yet been fully achieved. Even the basic question of which parts of the observed spectrum are due to the conduction band degrees of freedom is still not settled⁸⁻¹⁰. We show here that a comparison of the data to the theoretically calculated magnitude and temperature dependence of optical spectral weight, and of its relationship to T_c can resolve this issue. Our results indicate that several previous analyses^{8,9} underestimate the actual conduction band spectral weight, and suggest that a previous paper by several authors including one of us¹⁰ misidentified a key feature in the data. This misidentification arose pri-

marily from reliance on a theoretical calculation based on inappropriate system parameters.

In this paper we perform a systematic and quantitative comparison of the predictions of double-exchange-only models to data. We incorporate "real materials" aspects via a tight-binding fit to the band structure; in these materials a simple nearest neighbour hopping model represents the real material parameters adequately. In particular, we show that the crucial quantity for comparison of calculations to data or to other calculations is the conduction-band kinetic energy, a local expectation value related to the electron hopping amplitude and defined more precisely in Eq. (2). Because this kinetic energy is a local quantity, it can be easily and reliably calculated and is insensitive to the fine details of the band structure. When expressed in terms of the kinetic energy, the apparently disparate results of a variety of computations are seen to be in quantitative agreement. More importantly, because the kinetic energy may be determined from optical conductivity experiments^{13,14}, our results enable a detailed comparison of theory to experiment.

To treat the many-body physics of double-exchange, we use the highly successful dynamical mean-field method¹⁵. This provides a detailed and apparently reliable treatment of the local correlations which are crucial to the conclusions we wish to draw. We will argue that the effect of the omitted physics, which has to do with intersite fluctuations, may be reliably estimated for the issues of interest to us and is not too large.

The application of the dynamical mean-field method to double-exchange systems was pioneered by Furukawa³, whose important work established the basic usefulness of this method and presented many valuable results concerning the phase diagram, conductivity and other properties. However, his work was incomplete in some respects, incorrect in some details, and in many cases employed physically irrelevant parameters. The full treatment we present here is therefore needed.

We believe that the analysis presented in this paper may be useful in the general context of the development of a predictive theory of dynamical and ordering phenomena in systems, such as transition metal oxides, with strong interactions. This is an important goal of electronic condensed matter physics; and recent advances in computational power and in the techniques of many-body physics suggest that it may be obtainable. The dynamical mean field method¹⁵ seems particularly promising in this respect. It is computationally tractable, includes incoherent and inelastic effects, and can be combined with conventional band theory. Investigations of the extent to which this method is useful in the computation of real materials properties are urgently needed. The work described below is such an investigation. In this context we point out that one of the great advances in the theory of equilibrium critical phenomena arose from a careful and detailed application of mean-field theories. We believe that a similar opportunity may be present in the application of the dynamical mean field theory to strong

correlation physics.

The rest of the paper is organized as follows. Section II defines the double-exchange-only model, and explains how its parameters should be defined and related to experiments. Section III presents the dynamical mean-field formalism. Section IV presents the numerical and analytical results for the phase diagram, and corrects what seems to be a minor error in the phase diagram proposed in⁷. Section V presents results for the spectral weight (integrated area) in different regions of the optical conductivity spectrum. Section VI provides a summary of our theoretical results and a detailed interpretation of experimental data, particularly of optical conductivity and its relation to T_c . Readers interested only in this aspect may proceed directly to this section. Section VII is a conclusion and presents some possible directions for future research.

II. MODEL

The double-exchange-only (DE) model involves electrons (with orbital indices a, b) moving in a band structure defined by a hopping matrix t_{ij}^{ab} and a chemical potential μ , and connected by a Hund's coupling ($J > 0$) to core spins \mathbf{S} , which we take to be classical. We denote the operator creating an electron of spin α on orbital a of site i by $d_{i\alpha}^\dagger$ and define the double-exchange only Hamiltonian H_{DE} by¹⁶

$$H_{DE} = - \sum_{\langle ij \rangle, ab} t_{ij}^{ab} d_{i\alpha}^\dagger d_{j\beta\alpha} - \mu \sum_{i\alpha} d_{i\alpha}^\dagger d_{i\alpha} - J \sum_{i\alpha\beta} \vec{S}_i \cdot d_{i\alpha}^\dagger \vec{\sigma}_{\alpha\beta} d_{i\alpha\beta}. \quad (1)$$

Here t_{ij}^{ab} is the amplitude to hop from site i , orbital a to site j , orbital b . The calculated band structure²¹ is well fit by a t_{ij}^{ab} which involves only nearest-neighbour hopping.

A crucial quantity is the electron kinetic energy K , defined by

$$K = \frac{-2}{ZN_{sites}} \sum_{\langle ij \rangle} \langle t_{ij}^{ab} d_{i\alpha\sigma}^\dagger d_{j\beta\sigma} \rangle = \frac{2}{Z} \int \frac{d^d p}{(2\pi)^d} \epsilon_p^{ab} \langle d_{p\alpha}^\dagger d_{p\beta\alpha} \rangle, \quad (2)$$

where ϵ_p^{ab} is the dispersion obtained by Fourier transforming t_{ij}^{ab} , Z is the number of nearest neighbours and d is the spatial dimension. In the limit $J \rightarrow \infty$, K is the only relevant energy scale in the model and in particular the magnetic transition temperature T_c has been found to depend only on K ^{2,16,17}. K is also a suitable quantity for comparison to experiment because, in the physically realistic limit of nearest-neighbour hopping, K may be determined from an analysis of the optical

conductivity^{10,13}. We would like to mention that this K includes a sum over all bond directions and is 3 times larger than the K defined in Quijada et al.

III. FORMALISM

In this paper we study the magnetic transition temperature and kinetic energy of H_{DE} as functions of carrier density n and Hund's coupling using the dynamical mean field approximation, supplemented by an analytical treatment of the $J \rightarrow 0$ limit and by comparison to results of Monte Carlo⁷ and series expansions¹⁸.

The dynamical mean field method has been discussed extensively elsewhere¹⁵ and therefore we omit formal details. This scheme was first obtained in the limit $d \rightarrow \infty$ with $t_{ij} \sim 1/\sqrt{d}$, and is often referred to as the infinite dimensional limit, but the central approximation is actually the neglect of the momentum dependence of the electron self-energy, Σ . While this becomes exact in the limit $d \rightarrow \infty$, it is quite a good approximation in $d = 3$ ¹⁵, where the momentum dependence of Σ is quite weak.

To make the importance of the neglect of momentum dependence clear and to establish notation we sketch a derivation of the dynamical mean field equations. A momentum independent Σ implies that all of the many-body physics may be derived from the local (momentum-integrated) Green's function \mathbf{G}_{loc} , defined by

$$\mathbf{G}_{loc}(\omega) = Tr \int \frac{d^d p}{(2\pi)^d} \mathbf{G}(p, \omega) \quad (3)$$

where the Green's function, a matrix in orbital (ab) and spin ($\alpha\beta$) space, is

$$\mathbf{G}(p, \omega) = [\omega + \mu - \epsilon_p^{ab} - \Sigma_{\alpha\beta}^{ab}(\omega)]^{-1}. \quad (4)$$

It is convenient to define the density of states summed over bands $N(\epsilon) = \sum_{\lambda} \int \frac{d^d p}{(2\pi)^d} \delta(\epsilon - \epsilon_p^{\lambda})$, where ϵ_p^{λ} are the eigenvalues of ϵ_p^{ab} . We shall be interested in the pseudocubic manganese perovskites in the doping regimes where orbital order is not important. For these materials $N_{\lambda}(\epsilon) = \int \frac{d^d p}{(2\pi)^d} \delta(\epsilon - \epsilon_p^{\lambda})$ is independent of λ ; thus we use $N(\epsilon) = n_{orb} N_{\lambda}(\epsilon)$, where we have introduced the number of orbitals n_{orb} . For the physically relevant case, $n_{orb} = 2$, but the case $n_{orb} = 1$ has been considered by other workers³, so we retain n_{orb} as a variable to facilitate comparisons. The local Green's function is then proportional to the unit matrix in ab space, $\mathbf{G} = G_{loc, \alpha\beta} \delta_{ab}$ and the coefficient is

$$G_{loc, \alpha\beta}(\omega) = \int d\epsilon N(\epsilon) \frac{1}{\omega + \mu - \epsilon - \Sigma_{\alpha\beta}(\omega)}. \quad (5)$$

G_{loc} depends only on frequency and is therefore the solution of a single-site problem. This problem is specified by a mean-field function $b_{\sigma}(\omega)$ which, in the model of present interest, is related to G_{loc} via^{3,17}

$$G_{loc, \alpha\beta}(\omega) = \int d^2 \vec{\Omega} \frac{P(\vec{\Omega})}{b_{\alpha\beta}(\omega) - J \vec{S} \cdot \vec{\sigma}_{\alpha\beta}}; \vec{\Omega} = \vec{S} / |\vec{S}| \quad (6)$$

with

$$P(\vec{\Omega}) = \frac{1}{Z_{loc}} \exp \left[\sum_n Tr \ln [b_{\alpha\beta}(i\omega_n) - J \vec{S} \cdot \vec{\sigma}_{\alpha\beta}] \right], \quad (7)$$

and Z_{loc} ensures that $\int d^2 \vec{\Omega} P(\vec{\Omega}) = 1$. The self-energy is defined by

$$\Sigma_{\alpha\beta}(\omega) = b_{\alpha\beta}(\omega) - G_{loc, \alpha\beta}^{-1}(\omega) \quad (8)$$

and the mean-field function $b_{\alpha\beta}(\omega)$ is fixed by the requirement that Eq. (3) holds with $G_{\alpha\beta}(p, \omega)$ defined by Eq. (4), Σ defined by Eq. (8) and G_{loc} by Eq. (6). Using the momentum independence of the self-energies within this mean-field theory, the electron kinetic energy (Eq. (2)) can be written as

$$\begin{aligned} K &\equiv \frac{2}{Z} T \sum_n \int \frac{d^d p}{(2\pi)^d} \epsilon_p Tr [\mathbf{G}(p, i\omega_n)] \\ &= \frac{2}{Z} T \sum_n Tr [G_{loc}(i\omega_n)]^2. \end{aligned} \quad (9)$$

In a ferromagnetic state with magnetization direction \hat{m} we have

$$b_{\alpha\beta}(\omega) = b_0(\omega) + b_1(\omega) \hat{m} \cdot \vec{\sigma}_{\alpha\beta} \quad (10)$$

($b_1(\omega) = 0$ in the paramagnetic state). If the spin axis is chosen parallel to \hat{m} then $b_{\alpha\beta}$ becomes a diagonal matrix with components parallel ($b_{\uparrow} = b_0 + b_1$) and antiparallel ($b_{\downarrow} = b_0 - b_1$) to \hat{m} .

The precise form of the equation for b_{σ} depends on the form of the density of states $N(\epsilon)$, but the important behaviour of the physical observables do not, as long as $N(\epsilon)$ has a finite second moment ($\int d\epsilon N(\epsilon) \epsilon^2 < \infty$). We perform our calculations on the Bethe lattice with a semi-circular density of states per orbital

$$N(\epsilon) = \frac{\sqrt{4t^2 - \epsilon^2}}{2\pi t^2}. \quad (11)$$

Here t is a bandwidth parameter; the full bandwidth of the non-interacting ($J = 0$) problem is $4t$. This corresponds to number of nearest neighbours $Z = 2d$, as $Z \rightarrow \infty$ with tZ fixed. For this $N(\epsilon)$, the self-consistent equations for the b_{σ} are

$$\begin{aligned} b_{\uparrow} &= i\omega_n + \mu + \int_{-1}^1 d(\cos\theta) P(\theta) \times \\ &\quad \frac{(-b_{\downarrow} + J \cos\theta)}{b_{\uparrow} b_{\downarrow} - (b_{\uparrow} - b_{\downarrow}) J \cos\theta - J^2} \\ b_{\downarrow} &= i\omega_n + \mu - \int_{-1}^1 d(\cos\theta) P(\theta) \times \\ &\quad \frac{(b_{\uparrow} + J \cos\theta)}{b_{\uparrow} b_{\downarrow} - (b_{\uparrow} - b_{\downarrow}) J \cos\theta - J^2} \end{aligned} \quad (12)$$

and the local Green's function (Eq. 6) can be written in terms of the mean-fields as

$$G_{loc}^\sigma(i\omega_n) = i\omega_n + \mu - b_\sigma(i\omega_n). \quad (13)$$

The self energies are evaluated using Eq. (8) and the full Green's function from Eq. (4).

We will also be interested in the optical conductivity, σ . The contributions to σ from the states described by H_{DE} are obtained by coupling an electromagnetic field to H_{DE} (Eq. 1) via the Peierls coupling $t_{ij} \rightarrow t_{ij}e^{iA(r_i-r_j)}$ and performing linear response. If the self-energy is momentum independent then there are no vertex corrections in σ^{23} and

$$\sigma_{ij}(i\Omega_n) = \frac{e^2}{i\Omega_n} \left[S(\infty) - \sum_\sigma \int \frac{d^d p}{(2\pi)^d} T \sum_m Tr \left[\gamma_p^i \mathbf{G}_\sigma(p, i\omega_m) \gamma_p^j \mathbf{G}_\sigma(p, i\Omega_n + i\omega_m) \right] \right] \quad (14)$$

where γ_p is the current operator determined by the Peierls substitution; it includes both intra and inter-band transitions within the manifold of conduction band states. Since we concentrate on materials with cubic symmetry, $\sigma_{ij} \sim \delta_{ij}$ and hereafter we suppress the spatial indices on σ .

This conductivity obeys the sum rule^{13,14}

$$S(\infty) = \frac{a^{d-2}}{e^2} \int_0^\infty \frac{2}{\pi} d\Omega \sigma(\Omega) = \sum_{i\delta ab\alpha} t_\delta^{ab} \delta^2 \left\langle d_{i\alpha}^\dagger d_{i+\delta b\alpha} + H.c. \right\rangle. \quad (15)$$

If the nearest neighbour hopping is dominant then $\int_0^\infty \frac{2}{\pi} d\Omega \sigma(\Omega) = \frac{e^2}{a^{d-2}} K$. The experimentally measured optical conductivity includes additional transitions not described by H_{DE} and obeys the familiar f-sum rule $\int_0^\infty \frac{2}{\pi} d\Omega \sigma(\Omega) = \frac{ne^2}{m}$, with n the total (conduction and valence) electron density and m the bare mass. Extracting the portion pertaining to the e_g electrons from the measured conductivity has been controversial. We will show below how to do this using the information on spectral weights we derive below. Here we concentrate on spectral weight defined in Eq. (15). The real part of the optical conductivity (Eq. 14) can be written as

$$\sigma(\Omega) = e^2 \sum_\sigma \int d\epsilon_k N(\epsilon_k) \varphi(\epsilon_k) \int \frac{d\omega}{\pi} \frac{f(\omega) - f(\Omega + \omega)}{\Omega} \times A_\sigma(\epsilon_k, \omega) A_\sigma(\epsilon_k, \Omega + \omega) \quad (16)$$

where $A_\sigma(\epsilon_k, \omega) = -\frac{1}{\pi} Im G_\sigma(\epsilon_k, \omega)$ is the spectral function, $N(\epsilon_k)$ the density of states (Eq. 11) and $\varphi(\epsilon_k) = (4t^2 - \epsilon_k^2)/3$ is the current vertex for the Bethe lattice. We obtain $\varphi(\epsilon_k)$, the form of which for the Bethe lattice has not been given before (Ref.¹⁹ presents φ for the Gaussian density of states), by requiring that K be given

both by the explicit integration of σ (Eq. 16) and by the generally valid expression

$$K = \int d\epsilon_k \frac{d\omega}{\pi} f(\omega) \epsilon_k N(\epsilon_k) Im G(\epsilon_k, \omega). \quad (17)$$

Requiring the two to be equal yields the differential equation

$$-\frac{\partial}{\partial \epsilon_k} [N(\epsilon_k) \varphi(\epsilon_k)] = N(\epsilon_k) \epsilon_k, \quad (18)$$

the solution of which yields $\varphi(\epsilon_k)$.

IV. NUMERICAL METHODS

We now outline the numerical methods used to solve Eqs. (12) and compute physical quantities. For computational convenience, we rewrite the self-consistency Eqs. (12) in terms of b_0 and b_1 defined in Eq. 10. At $T > T_c$, there is no magnetic order and $b_1(\omega) = 0$. At $T = 0$ and non-zero J , all spins are ferromagnetically aligned implying $P(\theta) \rightarrow \delta(\cos\theta - 1)$, and one can analytically solve for the $b_{0,1}(i\omega_n)$ from Eq. (12). We initialize $b_{0,1}$ with the $T = 0$ expressions, and solve Eq. (12) on the Matsubara axis by direct iteration.

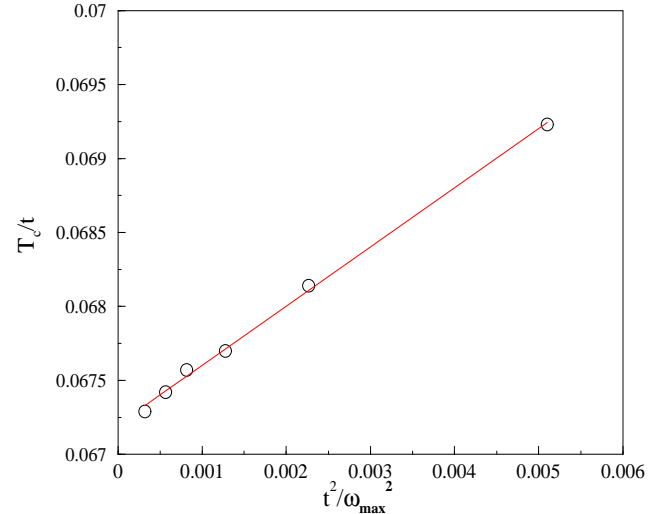


FIG. 1. The dependence of T_c on the Matsubara cutoff ω_{max} , for $n = 0.75$, $n_{orb} = 1$ and $J = 10t$; ω_{max} ranges from $(4t + J)$ to $4(4t + J)$. The quadratic dependence on t/ω_{max} holds for the $n_{orb} = 2$ as well. For our calculations we choose $\omega_{max} = 3(4t + J)$ which produces a value of T_c that is within 0.5% of the $\omega_{max} \rightarrow \infty$ value.

It is convenient to compute $P(\theta)$ by solving Eq. (12) on the Matsubara points, and then use this converged $P(\theta)$ to solve the equations on the real axis. Convergence to within an rms error of 10^{-4} was usually achieved within 12 iterations unless one is close to the magnetic T_c where there is critical slowing down. The electron density n and the normalized magnetization density m are given by

$$n = n_{orb} T \sum_n \left[G_{loc}^\uparrow(i\omega_n) + G_{loc}^\downarrow(i\omega_n) \right] \quad (19)$$

$$m = \int_{-1}^1 d(\cos\theta) \cos\theta P(\theta). \quad (20)$$

An accurate value of the transition temperature T_c was most conveniently obtained by computing values of m (Eq. 20) in the range $0.17 \leq m \leq 0.3$ and finding T_c by fitting to the mean-field expression $m^2(T) = \alpha(T_c - T)$, with α and T_c fit parameters.

The next issue is that of the number of Matsubara points needed to compute $S_{loc}(\theta)$, n and K . At large ω_n , the asymptotics of the mean fields are

$$\begin{aligned} b_0 &= i\omega_n + \mu - \frac{1}{i\omega_n + \mu} - \frac{1 + J^2}{(i\omega_n + \mu)^3} \\ b_1 &= \frac{Jm}{(i\omega_n + \mu)^2}. \end{aligned} \quad (21)$$

In our computations we choose a frequency cutoff ω_{max} and evaluate higher frequency contributions analytically using the asymptotic form given in Eq. (21). The errors in physical quantities are of order ω_{max}^{-2} . This is illustrated for T_c in Fig. 1. To achieve an accuracy of 5×10^{-4} in n , it was required to choose $\omega_{max} \geq 3(4t + J)$. Choice of this value of ω_{max} also ensures that the value of T_c is within 0.5% of the $\omega_{max} \rightarrow \infty$ value.

V. FERROMAGNETIC TRANSITION TEMPERATURE

A. Analytical results

We first present mean field results and establish the phase diagram, then show how to incorporate fluctuation corrections. We begin with analytical results for small ferromagnetic J . At $T = 0$ the core spins are magnetically ordered with a characteristic wavevector \vec{q} . The polarized core spins produce an effective magnetic field on the conduction electrons which polarizes them, leading to a magnetization \vec{m}_q and to a change in energy, which for small J is

$$\delta E = \frac{1}{2} (\chi_q^0)^{-1} \vec{m}_q \cdot \vec{m}_{-q} + \frac{1}{2} J (\vec{S}_q \cdot \vec{m}_{-q} + H.c) \quad (22)$$

where χ_q^0 is the magnetic susceptibility for noninteracting electrons at wavevector \vec{q} . Minimization of Eq. (22) leads to $\vec{m}_q = \chi_q \vec{S}_q$ and $\delta E = -\frac{1}{2} J^2 S_q^2 \chi_q$. Thus at small J the system will order at the wavevector which maximizes χ_q .

The wavevector at which χ is maximal depends on band filling and dimensionality. Here, for consistency and to facilitate comparison to other work^{3,7} we restrict ourselves to infinite- d . For very large d , $\chi(q)$ is independent of q except for regions of width $O(1/\sqrt{d})$ about $\vec{q} = 0$ and the commensurate antiferromagnetic vector

$\vec{q} = \vec{Q} = (\pi, \pi, \dots)$; therefore at $d = \infty$ we need to consider $\chi_{q=0}, \chi_{q=Q}$ and the susceptibility at a typical q , χ_{loc} ¹⁵. Fig. 2 shows the ferromagnetic (bold line), antiferromagnetic (solid line) and local (dashed line) susceptibilities for $J = 0$ calculated for a semicircular density of states. The phase corresponding to the maximal χ is the small J ground state. For $0 \leq n/n_{orb} \leq 0.195$, $\chi(q=0) \geq \chi_{loc}, \chi_Q$; this is the range of dopings where the DE model has a low J ferromagnetic ground state. At small J and intermediate n ($0.195 < n/n_{orb} < 0.35$), χ_{loc} is largest, implying order at wavevector different from both 0 and Q . At $d = \infty$ all such wavevectors are degenerate, implying some sort of highly degenerate ground state. Finite d corrections will select a particular wavevector. We therefore identify the phase as incommensurate (IC). For $n/n_{orb} > 0.35$, χ_Q is largest and the small J phase is a commensurate antiferromagnet.

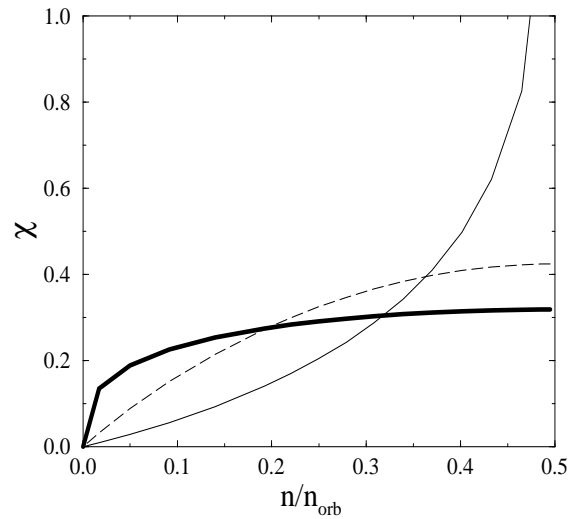


FIG. 2. The susceptibilities $\chi(q=0)$ (bold line), χ_{local} (dashed line) and $\chi(q=(\pi, \pi, \dots))$ as a function of the filling. The $J = 0$ ground state is ferromagnetic where $\chi(q=0)$ is largest, incommensurate where χ_{local} is largest, and commensurate antiferromagnetic where χ_Q is largest.

Using mean field theory, we may also obtain an expression for T_c . For finite range interactions, mean field theory is strictly correct only in the limit $d \rightarrow \infty$. We will consider finite d corrections below. Writing Eq. (22) in real space, focussing on a single site i , integrating out the conduction electrons and making a mean field ansatz yields a self-consistent equation for the polarization on site i . For example, for a ferro- or commensurate antiferromagnetic ordering, the effective field at site i , $h_{eff,i} = J \sum_{i \neq j} \chi_{i-j} \langle S_j \rangle$, has magnitude independent of i and we find

$$T_c = \frac{J^2}{3} [\chi_Q - \chi_{loc}]. \quad (23)$$

An explicit analytic expression for ferromagnetic T_c can be obtained by working out the susceptibilities in the mean-field Eq. 23 for $Q = 0$, and one finds that

$$T_c = \frac{J^2}{9\pi t}(\mu^2 - 1)\sqrt{4 - \mu^2}. \quad (24)$$

We observe $T_c \rightarrow 0$ at $\mu = 1$ which corresponds to $n = n_c = 0.195$; for $n > n_c$, the small J ground state becomes IC.

Next we consider the case of very large J , focussing first on the ground state energy. For $J > J^*(n)$, a ferromagnetic state would be fully spin polarized, and the ground state energy is simply that of the appropriate density of spin polarized electrons moving in the relevant band structure, and is therefore of order t . If $n/n_{orb} = 1$ the band is completely full, and the ground state energy vanishes, because no hopping is possible. For the semicircular density of states, $J^*(n_{orb}) = 2t$ and if $n = n_{orb}(1 - x)$ the the ground state energy E_{FM} is

$$E_{FM} = -2xt + O(x^2t). \quad (25)$$

At $n = n_{orb}$, a commensurate antiferromagnetic state is favoured, because virtual hops between the up and down sublattices leading to an energy gain $\sim -t^2/J$ are possible. For the Bethe lattice with Z nearest neighbours and near neighbour hopping t_δ , the energy is

$$E_{AF} = -\frac{2Zt_\delta^2}{J} \rightarrow -\frac{2t^2}{J} - O(x^2t) \quad (26)$$

where the arrow indicates the $d \rightarrow \infty$ limit. Further, one may consider an incommensurate state which for the purpose of $d = \infty$ energetics has a random spin arrangement, leading to

$$E_{IC} = -\frac{t^2}{J} - \sqrt{2}xt + O(x^2t). \quad (27)$$

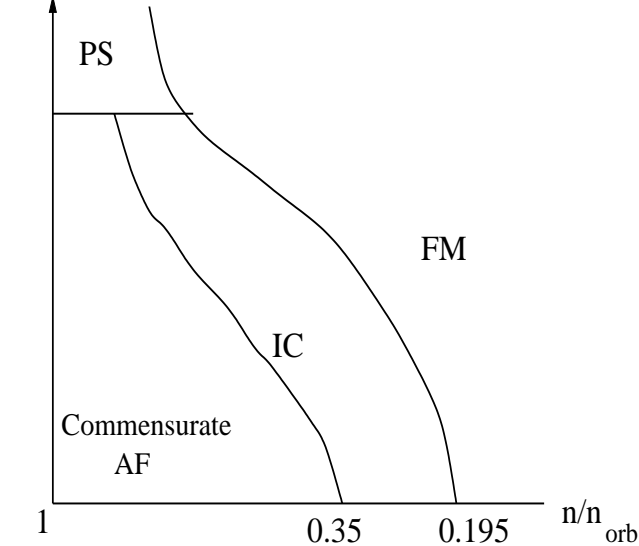


FIG. 3. The phase diagram of the double exchange model, as deduced from the analytic arguments at small and large J . At small J , one can have ferromagnetic (FM), commensurate anti-ferromagnetic (AF) or incommensurate (IC) phase. At large J , the IC phase is not energetically favoured and PS indicates phase separation between AF and FM.

Equating E_{FM} to E_{IC} implies a ferromagnet-incommensurate transition at $x_{F-I} = t/((2 - \sqrt{2})J)$; equating E_{AF} to E_{IC} yields incommensurate-antiferromagnetic transition at $x_{I-A} = t/(\sqrt{2}J)$. Thus at small $1 - n$ the sequence of spatially homogeneous phases as was also found at small J and small n . However, at small $1 - n$ and large J , inhomogeneous phases are favoured: the standard Maxwell construction applied to Eqs. (25,26,27) shows that in this model, which neglects long ranged Coulomb interactions, the whole small x and large J regime is in fact phase separated into commensurate AF and F with $x \sim 1/2$, as previously noted by⁷. Combining the small J and large J results, we obtain the phase diagram shown in Fig. (3). The qualitative behaviour is correct; we do not have precise numerical values for the IC-AF or PS phase boundaries.

We emphasize that the large- J antiferromagnetism and phase separated behaviour is tied to the regime $n \approx n_{orb}$, where the conduction band of the ferromagnetic state is almost completely full. The physically relevant regime for the manganites is $n < n_{orb}/2$, where the large J behaviour is simply ferromagnetic. Several published papers³ have asserted that behaviour associated with the regime $n \approx n_{orb}$ is relevant to the manganites. In our view, these assertions are unjustified because $n_{orb} = 2$, so the physical density corresponds to $n/n_{orb} < 0.5$.

It is possible that additional interactions, neglected here, could change the effective orbital degeneracy from 2 to 1. We do not believe this happens in the manganites. In support of our view we cite the case of LaMnO_3 . This is an insulator which has a frozen Jahn-Teller distortion which acts to quench the orbital degrees of freedom. This material is a $(0,0,\pi)$ antiferromagnet: its magnetic structure is ferromagnetic planes antiferromagnetically coupled. The ferromagnetic in-plane coupling means that virtual hopping to the empty orbital is the dominant process. The much weaker antiferromagnetic bond perpendicular to the plane is believed to be due to an additional $t_{2g} - t_{2g}$ superexchange which becomes important because the Jahn-Teller order strongly suppresses the out of plane hopping. In other words, even in the material in which the tendency to quench the orbital degree of freedom is strongest, there is no conduction band mediated antiferromagnetism in the physically relevant regime. We believe, therefore, that the physics of $n \approx n_{orb}$ is simply not relevant to the manganites, in contrast to the assertions made in⁷.

In the same way, the phase separation discussed in Refs.⁷ is crucially dependent on the existence of a commensurate antiferromagnetic order; the $(0,0,\pi)$ order observed in the actual materials would not lead to the same sort of phase separation, because it would permit metallic in-plane conduction.

B. Numerical results

By solving the dynamical mean field equations numerically, we have computed the ferromagnetic transition temperature T_c as a function of the Hund's coupling. Fig. 4 shows ferromagnetic T_c vs J for fillings of $n = 0.7$ (solid circles) and $n = 0.25$ (squares), for doubly degenerate e_g orbitals ($n_{orb} = 2$; $n/n_{orb} = 0.35$ or 0.125). As we noted in the analytic treatment of the low J limit, for not too low densities ($n > 0.2n_{orb}$), a ferromagnetic solution cannot be sustained. Thus for a modest n , as J is decreased the ferromagnetic T_c vanishes and the ground state changes from ferromagnetic to incommensurate to antiferromagnetic. As noted previously, we find $n_c \approx 0.195n_{orb} \approx 0.2n_{orb}$. We therefore suspect that the $n = 0.2(n_{orb} = 1)$ curve in the $T_c - J$ diagram of Ref.³, which indicates that T_c drops to 0 at a finite J of order 1, is incorrect at the low J end; the FM solution should be sustainable down to a very small J .

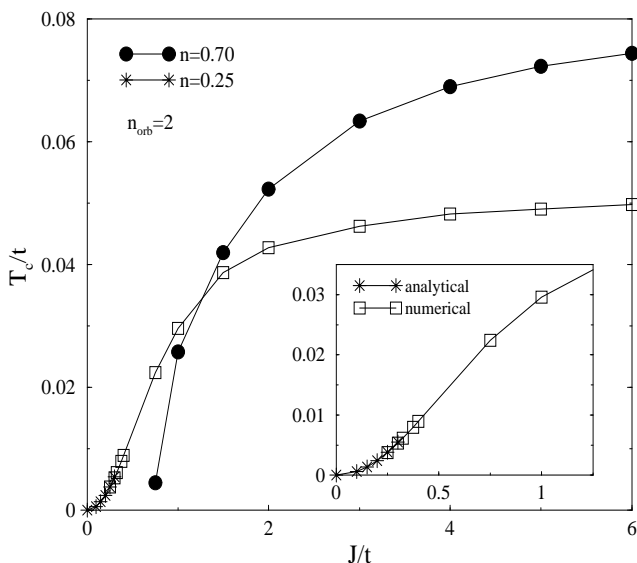


FIG. 4. T_c vs J plot of the double-exchange model for doubly degenerate e_g orbitals. The $n = 0.7$; $n_{orb} = 2$ curve is relevant for $\text{La}_{0.7}\text{A}_{0.3}\text{MnO}_3$ compounds. For $n \leq 0.39$, the model can sustain a ferromagnetic solution down to the lowest J . The inset amplifies the low J end of the $n = 0.25$ curve, to illustrate how the numerics (open boxes) patch on to the analytical expression (stars) from Eq. (24). The solid lines are a guide to the eye. $T_c(J = \infty) = 0.079$ for $n = 0.7$ and 0.055 for $n = 0.25$.

The stars in Fig. 4 correspond to Eq. (24), with the chemical potential $\mu = -1.52t$ for $n = 0.25$; $n/n_{orb} = 0.125$ (the curve is magnified in the inset). We notice that one cannot sustain a ferromagnetic transition for $n = 0.7$ as $J \rightarrow 0$.

The ferromagnetic transition temperature has an apparently complicated dependence on interaction strength and doping. We now show that this seemingly complicated dependence simply reflects the variation of the ki-

netic energy, K , with these parameters. Fig. 5 plots T_c against the change in kinetic energy between the paramagnetic and the $T = 0$ ferromagnetic state ($\Delta K = K(0) - K(T_c)$), both being normalized by the K of the noninteracting ($J = 0$) system at $T = 0$.

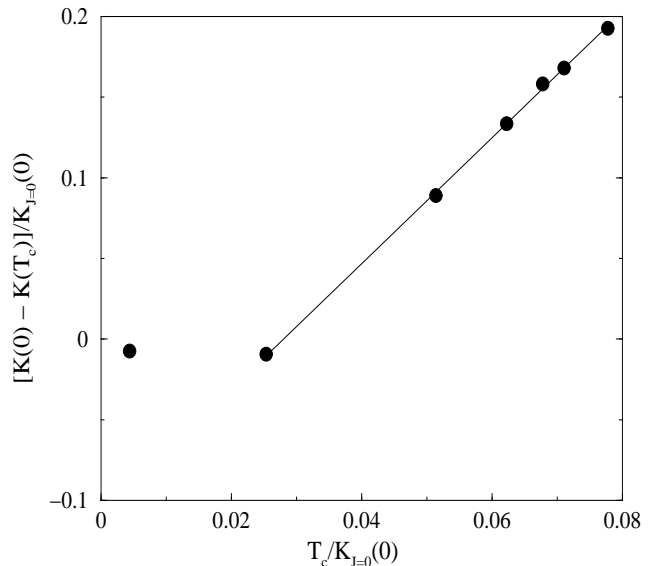


FIG. 5. $\Delta K = K(0) - K(T_c)$ vs. T_c for the DE model for $n = 0.7$; $n_{orb} = 2$. Both the quantities are scaled with the K for the non-interacting system at $T = 0$ ($K_{J=0}(T = 0) = 1.01t$ for $n = 0.7$).

To understand this curve, consider the general expression for the free energy, $F = E - TS$ of H_{DE} (Eq. 1), where S is the entropy and $E = -K - \mathcal{J}$ where K is given by Eq. (2) and

$$\begin{aligned} \mathcal{J} &= \sum_{i,\alpha,\beta} J \langle \vec{S}_i \cdot d_{i\alpha}^\dagger \vec{\sigma}_{\alpha\beta} d_{i\beta} \rangle \\ &= T \sum_n \ln [b_{n,\sigma} - J\sigma]. \end{aligned} \quad (28)$$

where the latter expression is the dynamical mean-field result. Entropy favours the disordered state; ferromagnetic order is driven by a decrease in energy. $T_c > 0$ implies $E_{fm} < E_{nm}$, where E_{fm} is the ground state energy of the ferromagnet and E_{nm} that of "non-ferromagnet" (incommensurate or antiferromagnetic order). At low T all spins are aligned, and carriers can move freely, while at high T the random spin arrangement and large J means carrier hopping is somewhat blocked. T_c is therefore set by the change in $K(T_c)$, which is a simple number ($\approx 1/3$) of $K(T = 0)$ as $J \rightarrow \infty$.

As $J \rightarrow \infty$, the local spin is always parallel to the core spin and \mathcal{J} does not change between ferromagnetic and paramagnetic states. The transition is entirely driven by the change in K between the paramagnetic and ferromagnetic states. In the non-ferromagnetic (NM) phase the band is narrower than in the FM phase, but at finite J the electron has some possibility to hop onto the "wrong" spin site. This is equivalent to the on-site mag-

netization not being saturated in the NM phase, thus $\mathcal{J}_{fm} > \mathcal{J}_{nm}$. Since $T_c \sim E_{nm} - E_{fm} = \Delta K + \Delta \mathcal{J}$, it implies that $E_{fm} = E_{nm}$ when $T_c = 0$ and we get $K_{fm} < K_{nm}$ at this point. So at high J , we start with fully polarized bands and with the magnetic state having more kinetic energy. The high J expansion suggests that everything comes from virtual hops : $\Delta K \sim t^2/J$ and $\Delta \mathcal{J} \sim J\Delta n \sim J \cdot t/J \sim t$. Since $\Delta \mathcal{J}$ is independent of J at large J , T_c is linear in ΔK for large values of J . As we reduce J to a value where the polarization isn't complete, first K 's cross and then $T_c \rightarrow 0$. We have used the dynamical mean-field equations to determine the points at which $E_{fm} = E_{nm}$ in Fig. 3. For $n = 0.7$ ($n/n_{orb} = 0.35$) the critical $J \approx 0.6t$.

Since K is of crucial interest to us, we present its values at $T = 0$ for the soluble limits $J = 0, \infty$ in Table I for a variety of fillings. At $J = 0$ the system is always paramagnetic, and the kinetic energy increases with n in the range $0 < n < 1$. For $J = \infty$ however, the kinetic energy is maximal for $n = n_{orb}/2$. As $K(T_c) = K(0)/\sqrt{2}$ for $J = \infty$ and the transition temperature is tied to the kinetic energy (Fig. 5), T_c also is a maximum at the same filling, as has been noted in earlier works^{17,3}.

TABLE I. The kinetic energy K at $T = 0$, evaluated using a dynamical mean field method with a semicircular density of states, for $J = 0$ and $J = \infty$ at different fillings.

n/n_{orb}	$K(J=0)/n_{orb}$	$K(J=\infty)/n_{orb}$
0.125	0.2160	0.1958
0.25	0.3916	0.3248
0.35	0.5086	0.3889
0.50	0.6496	0.4244
0.75	0.7994	0.3248

We have argued that the kinetic energy is the crucial parameter determining T_c . To further substantiate this we show in Table II results obtained for $T_c(J \rightarrow \infty)$ by a variety of techniques in a range of models¹, expressed in terms of $K_{J=\infty}(T = 0)$. Roder et al.¹⁸ used a series expansion technique. Yunoki et al.⁷ have studied thermodynamic properties of the classical core-spin model in $d = 3$ with a single orbital nearest neighbour hopping using Monte Carlo on $6 \times 6 \times 6$ clusters. Calderon and Brey⁴ have performed similar Monte Carlo calculations on $4 \times 4 \times 4$ and $20 \times 20 \times 20$ lattices, and argued that Yunoki et al.⁷ underestimated T_c by a factor of ~ 1.6 . The results of Calderon et al. are in agreement with those of Roder et al. Note that in all calculations the doping dependence of T_c is essentially the doping dependence of the kinetic energy.

We now consider the dynamical mean field results. These yield somewhat higher T_c/K results, as expected because fluctuations are neglected. Calderon and Brey partitioned the hopping term t_{ij} into average (\bar{t}) and random ($\delta t_{i,j}$) components and argued that fluctuations lead to a $\approx 25\%$ correction to T_c . Applying this cor-

rection leads to the numbers given in brackets, which are in good agreement with those found in Refs.^{4,18}.

TABLE II. $T_c/K(T = 0)$ for $J = \infty$; comparison of the different methods. The bracketed terms for $d = \infty$ indicate T_c values that are $\sim 25\%$ fluctuation corrected.

Method	n/n_{orb}	$T_c/K_{J=\infty}(T = 0)$
$d=\infty$	0.5	0.070(0.053)
$d=\infty$	0.25	0.063(0.050)
Series ¹⁸	0.5	0.053
Series ¹⁸	0.25	0.050
Yunoki ⁷	0.5	0.036
Yunoki ⁷	0.25	0.033
Calderon ⁴	0.5	0.056
Calderon ⁴	0.25	0.056

VI. OPTICAL CONDUCTIVITY

Next we discuss the optical conductivity of the double-exchange model. At large J the density of states of this model consists of two nearly semi-circular bands corresponding to conduction electrons parallel (\uparrow) and antiparallel (\downarrow) to the core spin. The bands are separated by an energy $2J$. This structure is shown in Fig. (6), which we now use to give a qualitative discussion of σ .

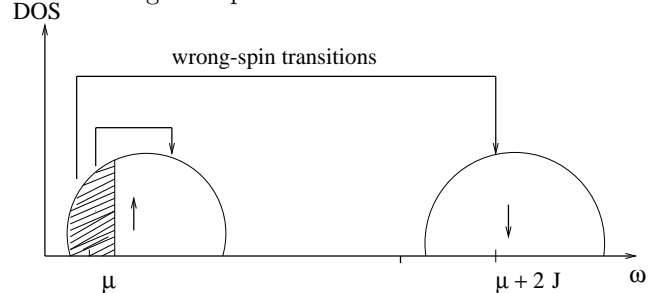


FIG. 6. The large J density of states, consisting of bands of electrons parallel (\uparrow) and antiparallel (\downarrow) to the core spin along with possible optical transitions indicated by arrows. μ denotes the chemical potential, and the shaded area represents the electron filling. There are two pieces to $\sigma(\omega)$; the transitions within the lower band with $\omega \sim t$ and the "wrong-spin" transitions from the lower to the upper spin band around $\omega \sim 2J$. The "wrong-spin" transitions become allowed as T is increased from 0. For large J , these two pieces are well separated.

The crucial point is that the optical process conserves electron spin. At $T = 0$ in the fully polarized ferromagnetic state all spins are aligned, making it impossible for an optical process to create a final state with an e_g electron anti-aligned to a core spin. Further, the perfect spin alignment means that no scattering processes are present; thus the $T = 0$ conductivity is simply given by the band theory of the spin polarized e_g electron manifold. The spectral weight in these transitions follows directly from

the band theory kinetic energy. Impurities, weakly coupled phonons etc. will change the form of the conductivity but will not significantly affect the total spectral weight.

As T is raised, the spin disorder increases, and an electron moved to an adjacent site may find itself anti-aligned to the new core spin⁸.

Thus as T is raised the resulting spin disorder leads to a broadening of σ , a decrease in total spectral weight, and also to a shift of oscillator strength to the peak at $\sim 2J$. For $2J \gg t$, the wrong-spin peak is well separated from the parallel spin transitions and we shall derive its spectral weight in this limit. Fig. 7(a) shows the real part of the optical conductivity (Eq. 16), calculated within the dynamical mean field theory, for the experimentally relevant filling of $n = 0.7$, for doubly degenerate conduction electrons. The results shown are for $J/t = 1, 2$ and 4 . The wrong-spin transitions produce the peak at $2J$, for $J > 1$ this becomes well separated from the same-spin transitions.

We are interested here in what fraction of the total optical weight goes into the wrong-spin transition. The spectral weight ratio is insensitive to details of the band structure. In what follows, we give an analytical estimate for the oscillator strength at $2J$ for large values of J and compare it with our numerical results. For $J \gg t$, $\Omega \sim 2J$ and $T = T_c$, the inter-band optical weight is

$$\int \frac{2}{\pi} d\Omega \sigma(\Omega) = \int d\epsilon_k N(\epsilon_k) \varphi(\epsilon_k) \int_{-\infty}^{\mu} \frac{d\omega}{\pi} A_-(\epsilon_k, \omega) \times \int_{-\infty}^{\infty} \frac{d\omega'}{\pi} \frac{A_+(\epsilon_k, \omega')}{J} \quad (29)$$

where we have used Eq. (16) for σ . Here, A_- is the imaginary part of the Green function for parallel electrons and A_+ for anti-parallel ones.

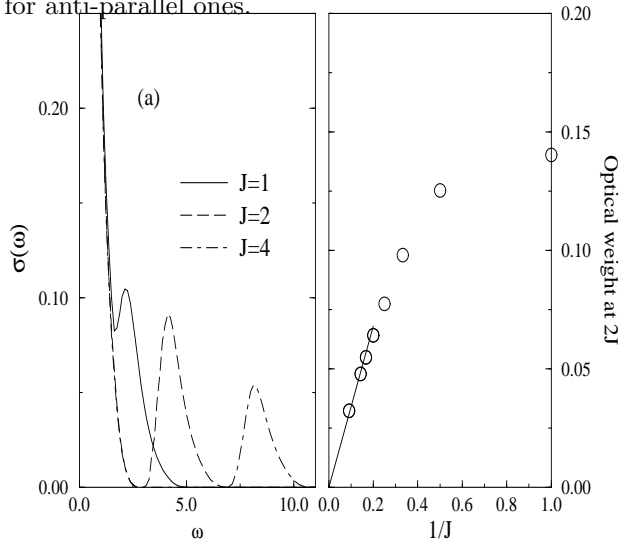


FIG. 7. (a) The optical conductivity at $T = T_c$ for the doubly -degenerate DE model for $n = 0.7$. The results shown are for $J = 1, 2$ and 4 ; the inter-band peak is at $2J$. (b) Spectral weight in the $e_g - e_g$ inter-band transitions, for $n = 0.7$ and $T = T_c$. For $J \gg t$, the inter-band weight falls off as $\frac{n}{J}$. The straight line has a slope of $n/2$, corresponding to the large J analytic expression Eq. (31).

Now, A_+ is an analytic function and its integral gives the real part evaluated at $\omega = J$, which is $1/(2J)$ in the large J limit. Thus

$$\int \frac{2}{\pi} d\Omega \sigma(\Omega) = \int d\epsilon_k \frac{(4 - \epsilon_k^2)^{3/2}}{12\pi J} \int_{-\infty}^{\mu} \frac{d\omega}{\pi} A_-(\epsilon_k, \omega). \quad (30)$$

The ω -integral gives the momentum space occupancy $n(\epsilon_k)$. If the scattering is strong enough, this is just n . So, for large J and at the magnetic transition we get

$$\int \frac{2}{\pi} d\Omega \sigma_{2J}(\Omega) = \frac{n}{2J} \quad (31)$$

which falls off as $1/J$ and is proportional to the filling n . The numerical results are shown in Fig. 7(b); we see that the analytic value for the slope, $n/2 = 0.35$ (straight line) from Eq. 31 overlays the numerical curve for large values of J . This analysis shows that the spectral weight in the wrong-spin transitions depends crucially on n . A previous calculation of σ used an $n_{orb} = 1$ and $n = 0.7$. The resulting oscillator strength in the wrong-spin transition is therefore not applicable to manganites with $n/n_{orb} = 0.35$ (and indeed the oscillator strength in³ is larger than the one we calculated for the physical n/n_{orb} by a factor of two). To aid in comparison to experiments we give in Table. III the total $T = 0$ spectral weight, the total $T > T_c$ spectral weight and, for $T > T_c$, the spectral weight in the wrong-spin and same-spin transitions, calculated using the dynamical mean field theory for various values of J .

TABLE III. The total $T = 0$ spectral weight $K(0)$, the total $T > T_c$ spectral weight $K(T_c)$ and, for $T > T_c$, the spectral weight in the wrong-spin (K_{anti}) and same-spin (K_{par}) transitions for various values of J , and $n = 0.35n_{orb}$.

J	$K(0)$	$K(T_c)$	K_{anti}	K_{par}
1	0.7778	0.8060	0.1209	0.6850
2	0.7778	0.6994	0.1067	0.5926
3	0.7778	0.6541	0.0833	0.5707
4	0.7778	0.6291	0.0661	0.5629
5	0.7778	0.6136	0.0547	0.5588
6	0.7778	0.6030	0.0467	0.5562
7	0.7778	0.5952	0.0408	0.5543
11	0.7778	0.5778	0.0275	0.5502

VII. COMPARISON WITH EXPERIMENTS

A. Overview

In this section we relate our results to experiments. The measurements we analyse are the value of the ferromagnetic transition temperature and the magnitude and temperature dependence of the spectral weight (integrated area) in different regions of the optical conductivity spectrum. The physics issues we are able to clarify include the extent to which the double-exchange-only model describes the behaviour of the manganites, the proper interpretation of the optical spectrum, and the value of the Hund's coupling. The remainder of this section is organized as follows. In sub-section B we summarize our results in a manner suited to comparison to data, in sub-section C we outline what is known about the optical conductivity data, emphasizing the heretofore unresolved issues arising in interpretation of experiments and in sub-section D we present the comparison between our results and data.

B. Summary of theoretical results

We have studied the double-exchange-only model defined by Eq. 1. This model involves itinerant electrons hopping among sites of a lattice and coupled ferromagnetically to electrically inert core spins. No other interactions are explicitly included. This model captures some aspects of the CMR manganese perovskites and of other 'double-perovskite' systems²⁴; whether other physics is important is the subject of present debate^{17,5}.

The double-exchange-only model was shown to have two crucial parameters: the electron kinetic energy K defined in Eq. 2 and the itinerant electron-core spin coupling J . K is the expectation value of a local operator. It depends on parameters like temperature and J , but is insensitive to details of band structure. For the J values and carrier concentrations of physical relevance, the ground state is a fully polarized ferromagnet and $K(T = 0)$ is independent of J and in the double-exchange-only model may be computed via a simple band structure calculation. The value appropriate to $\text{La}_{0.7}\text{Sr}_{0.3}\text{MnO}_3$ is $K \approx 0.84\text{eV}$. We calculate T_c as a function of $K(T = 0)$ and J using a mean field method which treats local dynamics exactly¹⁵, and by comparison to published Monte Carlo calculations⁴ were able to estimate the corrections to T_c from non-mean-field spatially dependent fluctuations. The dynamical mean field results are often published in terms of a bandwidth parameter t ; the t corresponding to the band theory K is $t \approx 1.07\text{eV}$.

By comparing our results to those obtained by other techniques, we found that in the $J \rightarrow \infty$ limit $T_c/K(T = 0) \approx 0.16$, essentially independent of model details. For finite J , we found (for carrier concentrations relevant to

the CMR materials with ferromagnetic ground states) that T_c was linearly proportional to the change, ΔK , of K between T_c and $T = 0$. We further found that as $J \rightarrow \infty$, $\Delta K/K \rightarrow 1/3$; as J is decreased, ΔK decreases. At a critical J , $\Delta K = 0$ and below this J a ferromagnetic ground state cannot be sustained.

As previously noted, K is measurable in optical experiments, and therefore a quantitative test of the double-exchange-only model is possible and conversely constraints on optical conductivity may be extracted from measured T_c 's. The issues involved in this analysis will be treated in the next sub-section. To conclude the present sub-section we discuss the additional information concerning the strength of non-double-exchange interactions which may be obtained from the comparison of T_c and the measured $K(T)$.

We may represent the electronic energy of a solid, $E_{el} = -K + I$ where K was defined in Eq. 2 and I represents the expectation value of all interactions, including the J term and other interactions not included in the double-exchange model. In the rest of the discussion we assume J is large enough to have a spin-polarized ground state.

In the double-exchange-only model at $T = 0$, K is saturated and given by the band theory value (assuming spin-polarized electrons). As T is increased, the entropy driven spin-disorder leads to a reduction in K ; the change in K between $T = 0$ and $T > T_c$ depends on J , and becomes as large as $1 - 1/\sqrt{2} \sim 30\%$ in the $J \rightarrow \infty$ limit. Other interactions do not commute with K , and therefore change the electronic state in a way which reduces K . Thus, we argue that K cannot be greater than the spin-polarized band theory value, and that a $K(T = 0)$ appreciably less than this value indicates other interactions are important.

As temperature is increased from $T = 0$, spin disorder leads to a decrease in K and therefore to an increase in the relative strength of the interaction terms which in turn causes a further decrease in K . This self-consistent effect says that for a given J , the relative change $\Delta K/K$ in kinetic energy between T_c and $T = 0$ increases with increasing interaction strength. This physics was investigated in Ref.¹⁷ for $J = \infty$ in the particular case of electron-phonon interaction, but is expected to be more general. Further, because kinetic energy is what decides T_c , the interaction induced decrease in K must decrease T_c below the value predicted by double-exchange.

To summarize, the double-exchange-only model predicts a definite set of relationships between T_c , $K(T = 0)$, and the T -dependence of K and ΔK . These are summarized in Fig. 5 and Tables. III and IV.

Adding other interactions causes T_c and $K(T = 0)$ to decrease and ΔK to increase.

C. Optical conductivity

This subsection discusses the interpretation of optical conductivity data. As we have shown, the magnitude and temperature dependence of the spectral weight in the e_g contribution to the optical conductivity contains crucial information about the electron kinetic energy and Hund's coupling. In order to extract this information one must identify the e_g contribution to the measured conductivity, which is not straightforward because of the overlap between the e_g transitions of interest and processes involving other bands. In this subsection we analyze the issues arising in the interpretation of the measured conductivity, with emphasis on how our theoretical results can be used to resolve some of the difficulties in interpreting data.

The optical conductivity $\sigma(\omega)$ is the linear response function relating spatially uniform frequency dependent current $\vec{j}(\omega)$ to applied electric field $\vec{E}(\omega)$. In simple terms, the conductivity describes how electrons move in response to an electric field, and therefore contains information about interactions which may hinder this motion. In metals it is useful to distinguish between intra-conduction-band processes (those which involve scattering of electrons between conduction band states, which in many cases including the CMR manganites are the states of immediate physical interest) and other processes which involve scattering of electrons from conduction band states to other (empty) bands, from other (filled) bands to the conduction bands, or which do not involve the conduction bands at all. The other processes are usually called interband, but in the manganites there are two orbitals per unit cell and therefore some of the intra-conduction-band processes are, strictly speaking, interband.

In any event, one would like to extract from the measured conductivity the portions pertaining to transitions between the states of interest (in the manganite case, the intra-conduction-band processes) and analyse only these. However in many cases involving transition metal oxides it has not been clear how to separate the interesting conduction band contributions from other un-interesting processes. The CMR materials are a promising system in which to investigate this issue because the conduction band contribution to σ has a strong temperature dependence and a definite relation to T_c , which can be used to distinguish it from other contributions.

The main point is this: the double-exchange-only model predicts a definite relation between the $T = 0$ e_g oscillator strength and T_c . Interaction corrections only reduce T_c below the double-exchange value and K below the band theory value. Therefore the part of the optical spectrum assigned to the e_g electrons must contain at least enough kinetic energy to reproduce the observed T_c , but cannot contain more kinetic energy than predicted by spin-polarized band theory results.

A further constraint is provided by the change ΔK in

kinetic energy between $T = 0$ and T_c . For H_{DE} (Eq. 1), $\Delta K \leq 0.3K(T = 0)$ and the maximal value occurs as $J \rightarrow \infty$. Limited information is available concerning models with additional interactions, but published calculations for the double-exchange plus phonon problem at $J \rightarrow \infty$ ¹⁷ show that the fractional change $\Delta K/K(T = 0)$ can become slightly larger than 0.5, but the magnitude of ΔK is never much larger than the double-exchange-only value. This is useful because the change in optical spectral weight can be accurately measured, and the observed changes can with confidence be attributed to the e_g electrons of interest. A final constraint comes from the position and spectral weight of the "wrong-spin" transitions. The point is that as $T \rightarrow 0$, all of the spins are aligned in both the ground state and all states accessible from it via the optical matrix element. However, for $T > T_c$, the core spins are completely disordered and therefore when an electron hops (or is pushed via the optical matrix element) from one site to another it has a probability for landing in the "wrong-spin" configuration, i.e. with e_g electron anti-parallel to the core. The probability depends on the hopping matrix element (i.e. the $T = 0$ kinetic energy) and the value of J . This physics was first pointed out by Okimoto et.al⁸, who, however, obtained what we argue below was an incorrect value of J . We have determined the optical oscillator strength in this transition, as a function of $K(T = 0)$ and J . The oscillator strength has a strong dependence on carrier density not noticed in previous work.

D. Analysis of data

Optical conductivity has been measured in a wide range of manganites by several groups^{8,9,11,12}. Results are qualitatively similar, but there are substantial quantitative differences between results of different groups. Some of the differences seem to be experimental artifacts associated with surface preparation^{20,12}; others seem to relate to differences in physics among various members of the CMR family of materials. As we shall see, our results provide consistency checks which allow one to separate artifacts from intrinsic behaviour and to make some statements about the underlying physics.

To be concrete, we discuss the data of Quijada et.al¹⁰, who measured $\sigma(\omega, T)$ for three pseudo-cubic manganite films $\text{La}_{0.7}\text{Sr}_{0.3}\text{MnO}_3$ (LSMO), $\text{La}_{0.7}\text{Ca}_{0.3}\text{MnO}_3$ (LCMO) and $\text{Nd}_{0.7}\text{Sr}_{0.3}\text{MnO}_3$ (NSMO). The qualitative features of the data are (i) at $\omega \leq 3\text{eV}$, an absorption with a pronounced frequency dependence and an intensity that shifts to lower frequency and increases markedly as T is decreased from T_c to a low temperature, (ii) a strong feature centered at $\omega \approx 4\text{eV}$ with little apparent T -dependence, and (iii) a weak feature at $\omega \approx 3\text{eV}$, visible as a decrease in absorption intensity as T is decreased below T_c . The interpretations offered in Ref.¹⁰ was that (1) the integral of the low T conductivity between $\omega = 0$

and $\omega = 2.7\text{eV}$ was a good representation of the total low T conduction-band spectral weight, (2) that the strong feature at $\omega \approx 4\text{eV}$ was a Mn-O interband transition and (3) the weak feature at $\omega \approx 3\text{eV}$ was the "peak at J " (it is actually at $2J$ in our units, as in Fig. 7) due to "wrong-spin" transitions characteristic of the spin disordered state. This identification is controversial. Okimoto et al.^{8,9} identified a lower energy feature as the peak at J .

We begin our discussion with the "peak at J ". The identification offered by Okimoto et al.^{8,9}, implies $J \approx 0.75\text{eV}$ which is less than the dynamical mean field hopping $t = 1.08\text{eV}$ (this is derived from equating the dynamical mean field kinetic energy K to the band theory $K = 0.84\text{meV}$). Thus the J must be larger as a ratio of $J/t \approx 0.7$ would imply a ferromagnetic state cannot be sustained at $n/n_{orb} = 0.35$, in contradiction to experiment.

We now turn to the identification of Quijada et al.¹⁰, which corresponds to $J = 1.5\text{eV}$, i.e to $J/t \approx 1.38$ or a fluctuation corrected $T_c \approx 0.03t \approx 310\text{K}$, somewhat below the 350K observed for $\text{La}_{0.7}\text{Sr}_{0.3}\text{MnO}_3$. This casts doubt on the interpretation offered by Quijada et al. Further, the spectral weight observed by Quijada et al. in the "peak at J ", $K_{anti} = 34\text{meV}$ is about twice the spectral weight predicted by our calculation, using the Quijada J and the t inferred from band theory. We conclude that the feature observed by Quijada et al. is unlikely to be the "peak at J " and that the true Hund's coupling is probably larger so that the peak at J is outside the experimental range. At least one needs a value of $J \approx 2\text{eV}$ to reproduce the observed T_c using the band theory K .

We digress briefly on the question of the origin of the observed feature. It seems reasonable that it is caused by a shift of the energy of the Mn-O interband transition at 4eV , due to changes in the e_g band as T is varied through T_c (the leading edge of this transition is an excitation from a filled oxygen state to the Fermi level in the $e - g$ band). One possibility is the double-exchange induced shift in chemical potential, discussed in a different context in³. Unfortunately, for relevant dopings, the changes that we find for $J/t > 2$ are of the order of $1 - 2\%$, too small to explain the observed feature. An alternative possibility is a polaronic shift associated with a change in effective electron-phonon interaction^{17,22}, but this has not been studied in detail.

We now present a more detailed discussion of the remainder of the spectrum, proceeding on the assumption that the "peak at J " is not visible in the spectrum at $\omega < 4\text{eV}$, i.e $J \geq 2\text{eV}$ and that the total $T = 0$ e_g spectral weight is less than or equal to the band theory value $K = 280\text{meV}$. Referring to Fig. 6 of Quijada et al.¹⁰, one observes a change between T_c and $T = 0$ $\Delta K(\omega^*) = \int_0^{\omega^*} d\omega \sigma(T \rightarrow 0, \omega) - \sigma(T > T_c, \omega)$ in spectral weight of $0.1\text{-}0.13$ eV in LSMO, $0.1\text{-}0.12$ eV in LCMO and 0.1 in NSMO. Consider LSMO first: if a double-exchange only model described the physics, the total $T = 0$ spectral

weight would be at least $3\Delta K$, i.e $K(T = 0) > 0.3\text{eV}$. This is slightly greater than the band theory value. Now the T_c of LSMO is $\approx 350\text{K} \approx 0.1K(T = 0)$. Reproducing this T_c with $K(T = 0) = 0.3\text{eV}$ would require a J slightly less than 2eV . From Table. III we see that such a J/K would imply a change ΔK in spectral weight much smaller than observed. Similar, but more severe problems arise for the other materials, LCMO and NSMO. The double-exchange-only constraint $K(T = 0) \geq \Delta K$ implies $K(T = 0) \geq 0.3\text{eV}$ for these materials as well. The lower T_c 's ($\approx 270\text{K}$ for LCMO, $\approx 250\text{K}$ for NSMO) would then imply $J = 1.5 - 1.8\text{eV}$, again yielding a ΔK that is too small, and a "peak at J " visible in the spectrum.

We would like to add here that our values of K are a factor of 3 higher than that of¹⁰. This is because of the $1/\sqrt{d}$ dependence of each current vertex in the expression for $\sigma(\omega)$. Thus, for $d = 3$, the kinetic energies of Quijada et al should be multiplied by $(\sqrt{d})^2 = 3$ to compare with our numbers. We do this in Table IV for facilitate comparison.

To conclude this section we invert the logic, using the observed transition temperatures and ΔK to obtain bounds and estimates for the conduction band spectral weights. We argue that for a given $K(T = 0)$ and J , the double-exchange-only model gives an upper bound for T_c . Thus values of T_c and J yield a lower bound for $K(T = 0)$. These bounds are shown in the Table IV for $J = 2\text{eV}$, 3eV and 4eV for the systems studied by Quijada et al. Note that an upper bound of $K(T = 0)$ is given by the band theory value.

An alternative estimate may be obtained by considering the limit $J \rightarrow \infty$. In this case, as noted in¹⁷, T_c is a universal function of $K(T_c)$ (which may itself be affected by other interactions). Further, T_c must decrease as J is decreased; thus, we may obtain a lower bound on $K(T_c)$ from the $J = \infty$ result for T_c . These bounds are also listed in Table IV.

TABLE IV. The lower bounds on the kinetic energies (K_{min}) at $T = 0$ and T_c for the systems studied by Quijada et al., shown for $J = 2\text{eV}$, 3eV and 4eV . The upper bound is given by the band theory value $K_{band}(0) = 840\text{meV}$. To compare with experiments, we cite the values of Ref.¹⁰ in the last two rows. The experimental values for K are represented in the conventions of this paper, i.e. values from¹⁰ multiplied by 3. All energies are in meV.

	LSMO	LCMO	NSMO
$K_{min}(0); J = 2\text{eV}$	630	392	350
$K_{min}(0); J = 3\text{eV}$	535	336	327
$K_{min}(0); J = 4\text{eV}$	514	345	314
$K_{min}(T_c); J = \infty$	477	330	309
$K_{expt}(0)$	780	660	600
$K_{expt}(T_c)$	477	393	390

It is interesting to note that the experimental $K(T_c)$ for LSMO is 477meV , which exactly saturates the lower

bound on $K(T_c)$ from double-exchange. Because the infinite- J double-exchange-only T_c is expected to be the upper bound to the true T_c of an interacting model we expect that in the actual material the J is larger than $2eV$ (so the model is not far from the $J = \infty$ limit and we suspect that the integration up to $\omega = 2.7eV$ does not capture quite all of the spectral weight).

VIII. CONCLUSIONS

We have given a complete and correct treatment of the phase diagram, kinetic energy and some aspects of the optical conductivity of the double-exchange-only model of mobile carriers coupled to core spins. We have determined the physics operating in different regions of the phase diagram and have demonstrated the importance of choosing parameters (especially carrier density) appropriate to the materials of interest by exhibiting the incorrect results obtained by the use of wrongly chosen parameters. We have shown that the crucial quantity is the electron kinetic energy and have used our results to estimate the kinetic energy of several manganite systems. Our results also provide insight into the crucial question of which portions of the spectrum pertain to the low energy electronic degrees of freedom.

There are several directions for future work. One is to combine the dynamical mean field method with a realistic band structure, to obtain a treatment of the frequency dependence of σ . Another is to employ the methods presented here to models where double-exchange is combined with other interactions. If this were carried through, it seems likely that the combination of T_c and the changes in optical spectral weight could be analysed to provide detailed knowledge of the strength, energy scale, and nature of any additional couplings.

IX. ACKNOWLEDGEMENTS

We thank H.D. Drew, B.G Kotliar and H. Monien for helpful discussions and the University of Maryland MR-SEC and NSF-DMR-9705482 for support.

- ⁶ A. J. Millis, P. B. Littlewood, and Boris. I. Shraiman, Phys. Rev. Lett. **74**, 5144(1995).
- ⁷ S. Yunoki, J. Hu, A. L. Malvezzi, A. Moreo, N. Furukawa and E. Dagotto, Phys. Rev. Lett. **80**, 845(1998); E. Dagotto, S. Yunoki, A. L. Malvezzi, A. Moreo, J. Hu, S. Capponi, D. Poilblanc and N. Furukawa, Phys. Rev. B. **58**, 6414(1998).
- ⁸ Y. Okimoto, T. Katsufuji, T. Ishikawa, A. Urushibara, T. Arima, and Y. Tokura, Phys. Rev. Lett. **75**, 109 (1995).
- ⁹ Y. Okimoto, T. Katsufuji, T. Ishikawa, T. Arima, and Y. Tokura, Phys. Rev. B. **55**, 4206 (1997).
- ¹⁰ M. Quijada et al., Phys. Rev. B. **58**, 16093 (1998).
- ¹¹ K. H. Kim, J. H. Jung, and T. W. Noh, Phys. Rev. Lett. **81**, 1517 (1998).
- ¹² H. J. Lee, J. H. Jung, Y. S. Lee, J. S. Ahn, T. W. Noh, K. H. Kim and S-W. Cheong, cond-mat/9904173.
- ¹³ A. J. Millis and S. N. Coppersmith, Phys. Rev. B. **42** 10807 (1990).
- ¹⁴ D. Baeriswyl, C. Gros, and T. M. Rice, Phys. Rev. B. **35** 8391 (1987).
- ¹⁵ A. Georges, G. Kotliar, W. Krauth and M. J. Rozenberg, Rev. Mod. Phys **68**, 13 (1996).
- ¹⁶ K. Kubo and A. Ohata, J. Phys. Soc. Jpn **33**, 21(1972).
- ¹⁷ A. J. Millis, R. Mueller and Boris. I. Shraiman, Phys. Rev. B. **54**, 5405(1996).
- ¹⁸ H. Roder, R. R. P. Singh and J. Zang, Phys. Rev. B. **B56**,5084(1997).
- ¹⁹ E. Lange and G. Kotliar, Phys. Rev. Lett. **82**, 1317 (1999).
- ²⁰ K. Takenaka, K. Iida, Y. Sawaki, S. Sugai, Y. Moritomo and A. Nakamura, cond-mat/9905310 (to be published in Physica Status Solidi).
- ²¹ W. E. Pickett and D. Singh, Phys. Rev. B. **53**, 1146(1996).
- ²² A. J. Millis, R. Mueller and Boris. I. Shraiman, Phys. Rev. B. **54**, 5389(1996).
- ²³ G. D. Mahan, Many Particle Physics, Plenum Press (1990).
- ²⁴ K. -I. Kobayashi, T. Kimura, H. Sawada, K. Terakura, and Y. Tokura, Nature **395**, 677 (1998).

¹ See, e.g, Phil. Trans. Roy. Soc. **A376**, 1469-1712 (1998).

² C. Zener, Phys. Rev. **82**, 403 (1951); P. W. Anderson and H. Hasegawa, Phys. Rev. **100**, 675 (1955); P-G. de Gennes, Phys. Rev. **118**, 675(1960).

³ N. Furukawa , J. Phys. Soc. Jpn. **63**, 3214 (1994); N. Furukawa , J. Phys. Soc. Jpn. **64**, 32754 (1995); N. Furukawa , cond-mat/9812066.

⁴ M. J. Calderon and L. Brey, cond-mat/9801311.

⁵ E. Dagotto, Science **283**, 2034 (1999).